IEEE Access
Multidisciplinary | Rapid Review | Open Access Journal

Received November 19, 2020, accepted December 8, 2020, date of publication December 11, 2020,
date of current version December 29, 2020.

Digital Object Identifier 10.1109/ACCESS.2020.3044053

Uplink Null-Space Expansion for Multiuser Massive MIMO in Time-Varying Channels Under Unknown Interference

KABUTO ARAI[1], (Graduate Student Member, IEEE), KAZUKI MARUTA[2], (Member, IEEE), AND CHANG-JUN AHN[1], (Senior Member, IEEE)

[1]Graduate School of Engineering, Chiba University, Chiba 263-8522, Japan
[2]Academy for Super Smart Society, Tokyo Institute of Technology, Tokyo 152-8552, Japan

Corresponding author: Kabuto Arai (kabuto.arai@chiba-u.jp)

This work was supported in part by the KDDI Foundation, in part by the Mazda Foundation, and in part by the KAKENHI Grant-in-Aid for Scientific Research (B) under Grant 20H04178.

ABSTRACT This article proposes a novel postcoding design scheme for suppressing inter-user interference (IUI) and inter-cell interference (ICI) in uplink multiuser massive multiple-input multiple-output (MIMO) system in time-varying channel environments. In the uplink system, the base station (BS) designs postcoding weight based on estimated channel state information (CSI) to suppress IUI. When user terminals move, the estimated CSI is outdated because actual channels vary with time. This causes IUI and leads to degrading the system capacity. Besides, ICI extensively arises in multiuser massive MIMO systems since many users are simultaneously supported in each cell. The accuracy of CSI estimates is degraded since ICI contaminates the uplink pilot sequences from desired users. Adopting a weight design based on minimum mean square error (MMSE) criteria, we can suppress ICI adequately, and exploiting plentiful degrees of freedom (DoFs) of massive array, we can also suppress IUI even in time-varying channels by steering many nulls for one user based on null-space expansion (NSE) scheme. The computer simulations clarify that the proposed scheme has superior SINR performance in Rayleigh fading channel at low speed, low SIR, and high SNR regions while it is effective at almost all conditions in Rician fading channel.

INDEX TERMS Inter-user interference, inter-cell interference, time-varying channel, multiuser massive MIMO, null-space expansion, sample matrix inversion.

I. INTRODUCTION

The spread of the number of mobile terminals such as smartphones, PCs, and tablets has led to an explosion in data traffic. Transmission bandwidth for wireless communication systems such as LTE or Wi-Fi has been widened in order to deliver such unlimitedly increasing demands. It causes the depletion of limited frequency resources. In the fifth-generation mobile communication (5G) and beyond, the millimeter-wave band is used to ensure wide bandwidth available [1], [2]. Although this advancement is inevitable, it requires a higher transmission power due to large propagation loss. In order to compensate for the shortcomings, massive array beamforming is a promising solution [3], [4] enabled by a huge number of antenna elements over a hundred on the base station (BS) side. A typical approach to making effective use of limited frequency resources is spatial multiplexing, i.e., (multiuser) multiple-input multiple-output (MIMO) [5], [6]. In multiuser MIMO communication, plural streams for respective user terminals are multiplexed at the same time and the same frequency. According to the 5G specification, up to 12 layers for multiuser MIMO are to be supported [7]. In a cellular-based uplink multiuser MIMO system, BS estimate channel state information (CSI) from the pilot signal transmitted by the desired user in the target cell. Based on the estimated CSI, BS designs a MIMO weight and can suppress inter-user interference (IUI) by steering nulls to the other desired users in the target cell. However, when users move, the channel state varies with time, and it causes a difference between the actual channel and the estimated CSI. Therefore, the MIMO weight designed by the estimated CSI is outdated, resulting in IUI [8].

To mitigate the effect of time variation, channel prediction techniques have been researched for the time-varying

The associate editor coordinating the review of this manuscript and approving it for publication was Hasan S. Mir.

channel environment [9], [10]. In [9], the channel prediction scheme based on the autoregressive (AR) model has been proposed. This method needs to compute the autocorrelation function of the time-varying channels based on many past estimated CSI. Therefore, AR-based prediction method has a high computation complexity. In [10], First-order Taylor expansion (FIT)-based channel prediction scheme has been proposed in time-varying massive MIMO environments. This method has low computational complexity because it uses only the first term of a Taylor series to approximate value for the time-varying channel. However, the prediction accuracy is slightly lower than AR-based prediction method because of the linear approximation that ignores the terms after the second-order of the Taylor series. The performance of a multiuser MIMO system in time-varying channels has been evaluated [8]. Designing the MIMO weight based on future predicted channels by past estimated CSI, IUI can be suppressed even in time-varying channel environments. However, channel estimation error due to receiver noise and inter-cell interference (ICI) was not considered. Besides, since these methods still steer only one null per one user, it causes IUI when the predicted channel is not appropriate compared to the actual channel.

To solve this problem, null-space expansion (NSE) scheme has been proposed as one of the outstanding interference suppression techniques [11], [12]. In this method, the IUI is suppressed by steering additional nulls based on the past estimated CSI. As a result, it has superior performance better than the channel prediction approaches.

Fundamental effectiveness of NSE is disclosed in downlink transmission. This article attempts to extend this concept to uplink reception. Here, NSE relies on deterministic CSI estimates to suppress intra-cell IUI. It cannot suppress unknown interference, such as ICI from adjacent cells. In general, ICI extensively arises in multiuser massive MIMO systems since many users are simultaneously supported in each cell [13]. ICI not only contaminates data transmitted by desired users in the target cell but also contaminates the pilot signal required for channel estimation. Therefore, it degrades the CSI estimation accuracy resulting in degradation of the IUI suppression capability [14]. Consider the uplink signal reception, the representative methods for suppressing unknown interference have been developed well known as least mean squares (LMS), recursive least squares (RLS), and sample matrix inversion (SMI) algorithms [15], in the adaptive array signal processing field. These methods enable to suppress the unknown interference by the postcoding weight based on the minimum mean square (MMSE) criteria. In the time-varying channel environment, interference suppression performance deteriorates since these methods use a known reference signal added at the beginning of the transmission data to design the postcoding weight. Considering the extension of NSE to the receiving end, it is possible to deal with unknown interference thanks to the excessive degree of freedom (DoF) provided by the massive array of BS.

A. RELATED WORK

Several developmental studies have been conducted, originating from the basic principles of NSE. An analytical consideration of the NSE principles was given, focusing on element waves [16] as well as antenna beam pattern [17]. Besides, an extension was made to the case where the user terminal is equipped with more than one antenna [18], [19]. It also concluded that NSE is a reasonable choice in terms of interference suppression performance and computation complexity. An experimental study through an indoor channel measurement was also carried out, and the feasibility was demonstrated [20], [21]. These works still focused on the downlink.

As for the data-aided interference suppression schemes related to massive MIMO systems, its main target is to overcome the pilot contamination problem. These methods are completely blind [22] or semi-blind [23], [24] approaches that utilize many received data in addition to the pilot signal in order to estimate both intra-cell and inter-cell CSI. However, these methods do not work properly in the time-varying channel environment since the statistical properties of the received signal change with time in the long data part.

B. CONTRIBUTION

Based on the above background, a joint application of NSE and adaptive algorithms brings us expectations to deliver a promising solution against the extensive co-channel interference problem. We address this issue to realize the effective and generic use of spectrum resources in mobile communications. The specific contributions of this article are as follows.

1) We consider an uplink multiuser massive MIMO system in which unknown interferences from adjacent cells arise in the time-varying channel environment.
2) We propose a postcoding weight design that suppresses both ICI and IUI for the system of interest. The weight is designed utilizing the past pilot signals and has the property of steering additional nulls for not only desired users in the target cell but also for interfering users in adjacent cells.

The organization of this article is as follows: Section II explains the signal transmission/reception model of multiuser massive MIMO in time-varying channels and the conventional schemes. Section III presents the proposed scheme based on NSE and MMSE-SMI for uplink interference suppression. Section IV discloses simulation results to verify the superiority of our proposal compared with performances of conventional schemes. Finally, this article is concluded in Section V.

II. SYSTEM MODEL AND CONVENTIONAL METHOD

In this article, we denote matrices and vectors by boldfaced capital letters and lowercase letters, respectively. Normal letters represent scalar quantities. $(\cdot)^*$, $(\cdot)^T$, and $(\cdot)^H$ indicate conjugate, transpose, and conjugate transpose, respectively. $|\cdot|$, $\|\cdot\|_{\mathrm{F}}$, and $\mathrm{tr}(\cdot)$ indicate absolute values, Frobenius

norm, and the trace, respectively. The expectation operator is denoted by E[·]. The element of matrix $\mathbf{A}$ at i-th row and j-th column is denoted by $a_{ij} = (\mathbf{A})_{ij}$. $(\cdot)^{\frac{1}{2}}$ is defined such that $\mathbf{A}^{\frac{1}{2}}(\mathbf{A}^{\frac{1}{2}})^H = \mathbf{A}$. If f is scalar function of matrix $\mathbf{A} \in \mathbb{C}^{M\times N}$, then its derivative is defined as

$$\frac{\partial f(\mathbf{A})}{\partial \mathbf{A}^*} = \begin{bmatrix} \frac{\partial f(\mathbf{A})}{\partial a_{11}^*} & \cdots & \frac{\partial f(\mathbf{A})}{\partial a_{1N}^*} \\ \vdots & \ddots & \vdots \\ \frac{\partial f(\mathbf{A})}{\partial a_{M1}^*} & \cdots & \frac{\partial f(\mathbf{A})}{\partial a_{MN}^*} \end{bmatrix}.$$

The submatrix of $\mathbf{A} = \begin{bmatrix}\mathbf{a}_1 & \cdots & \mathbf{a}_j & \cdots & \mathbf{a}_N\end{bmatrix}$, which excludes the j-th column vector $\mathbf{a}_j$ from the matrix $\mathbf{A}$ is defined as $\mathbf{A}_{\bar{j}} = \begin{bmatrix}\mathbf{a}_1 & \cdots & \mathbf{a}_{j-1} & \mathbf{a}_{j+1} & \cdots & \mathbf{a}_N\end{bmatrix}$. The subvector of $\mathbf{x} = \begin{bmatrix}x_1 & \cdots & x_i & \cdots & x_M\end{bmatrix}^T$, which excludes the i-th element x_i from the vector $\mathbf{x}$ is defined as $\mathbf{x}_{\bar{i}} = \begin{bmatrix}x_1 & \cdots & x_{i-1} & x_{i+1} & \cdots & x_N\end{bmatrix}$. We denote the identity matrix of size $N \times N$ as $\mathbf{I}_N$ and the all-zero matrix of size $M \times N$ as $\mathbf{O}_{M\times N}$. The primary notations used in the mathematical formulation are summarized in the Table 1.

TABLE 1. Notations of parameters.

Notation	Descriptuion
N_r	Number of BS antennas
N_d	Number of desired users
N_i	Number of interfering users
N_p	Number of pilot symbols
N_s	Number of data symbols
ρ_d^2	Transmission signal power of desired users
ρ_i^2	Transmission signal power of interfering users
σ_n^2	Receiver noise variance
v	User velocity
T_s	Symbol duration
Q	Number of past pilot sequences
K	Rician K-factor
$\mathbf{x}_\mathrm{d}[n,k] \in \mathbb{C}^{N_\mathrm{d}\times 1}$	Transmission signal vector from desired users at the n-th subframe and the k-th symbol
$\mathbf{x}_\mathrm{i}[n,k] \in \mathbb{C}^{N_\mathrm{i}\times 1}$	Transmission signal vector from interfering users
$\mathbf{y}[n,k] \in \mathbb{C}^{N_\mathrm{r}\times 1}$	Received signal vector
$\mathbf{H}_\mathrm{d}[n,k] \in \mathbb{C}^{N_\mathrm{r}\times N_\mathrm{d}}$	Uplink channel matrix for desired users
$\mathbf{H}_\mathrm{i}[n,k] \in \mathbb{C}^{N_\mathrm{r}\times N_\mathrm{i}}$	Uplink channel matrix for interfering users
$\mathbf{X}_\mathrm{d}^{(n)} \in \mathbb{C}^{N_\mathrm{d}\times N_\mathrm{p}}$	Known pilot signal matrix for desired users at the n-th subframe
$\mathbf{X}_\mathrm{i}^{(n)} \in \mathbb{C}^{N_\mathrm{i}\times N_\mathrm{p}}$	Unknown pilot signal matrix for interfering users
$\mathbf{Y}^{(n)} \in \mathbb{C}^{N_\mathrm{r}\times N_\mathrm{p}}$	Received pilot signal matrix
$\mathbf{H}_\mathrm{d}^{(n)} \in \mathbb{C}^{N_\mathrm{r}\times N_\mathrm{d}}$	Uplink channel matrix for desired users at pilot part of the n-th subframe
$\mathbf{H}_\mathrm{i}^{(n)} \in \mathbb{C}^{N_\mathrm{r}\times N_\mathrm{i}}$	Uplink channel matrix for interfering users at pilot part
$\hat{\mathbf{H}}_\mathrm{d}^{(n)} \in \mathbb{C}^{N_\mathrm{r}\times N_\mathrm{d}}$	Estimated channel matrix for desired users at pilot part of the n-th subframe
$\mathbf{W}^{(n)} \in \mathbb{C}^{N_\mathrm{r}\times N_\mathrm{d}}$	Postcoding weight matrix at the n-th subframe
$\mathbf{N}^{(n)} \in \mathbb{C}^{N_\mathrm{r}\times N_\mathrm{p}}$	Receiver noise matrix at pilot part of the n-th subframe
$\hat{\mathbf{x}}_\mathrm{d}[n,k] \in \mathbb{C}^{N_\mathrm{d}\times 1}$	Weighted received signal vector at the n-th subframe and the k-th symbol
$\mathbf{Y}_\mathrm{e}^{(n)} \in \mathbb{C}^{N_\mathrm{r}\times QN_\mathrm{p}}$	Extended received pilot signal matrix at the n-th subframe
$\mathbf{X}_\mathrm{de}^{(n)} \in \mathbb{C}^{N_\mathrm{d}\times QN_\mathrm{p}}$	Extended pilot signal matrix for desired users
$\mathbf{R}_{\mathbf{yy}}^{(n)} \in \mathbb{C}^{N_\mathrm{r}\times N_\mathrm{r}}$	Sample auto-correlation matrix of $\mathbf{y}$
$\mathbf{R}_{\mathbf{yx}_\mathrm{d}}^{(n)} \in \mathbb{C}^{N_\mathrm{r}\times N_\mathrm{d}}$	Sample cross-correlation matrix between $\mathbf{y}$ and $\mathbf{x}_\mathrm{d}$
$\mathbf{R}_{\mathrm{d}l} \in \mathbb{C}^{N_\mathrm{r}\times N_\mathrm{r}}$	BS side spatial correlation matrix for the l-th desired user
$\mathbf{R}_{\mathrm{i}m} \in \mathbb{C}^{N_\mathrm{r}\times N_\mathrm{r}}$	BS side spatial correlation matrix for the m-th interfering user

A. SYSTEM MODEL

This article evaluates the performance of uplink multiuser MIMO in which unknown interference from adjacent cells arises in the time-varying channel environment. System model and its signal transmission/reception process are illustrated in Fig. 1. We define desired users as who belonging to the target cell and interfering users as who belonging to adjacent cells, respectively. Let N_r, N_d, N_i denote the number of BS antenna elements, desired users, interfering users, respectively. Each user has one antenna and shares the same frequency. At BS side, using uplink pilot sequences, postcoding is performed for desired signal detection. We assume that pilot sequences from desired users are known but are unknown from interfering users. Therefore, BS can estimate CSI of the desired user but cannot do for the interfering users. Fig. 2 shows the frame structure defining the arrangement of pilot symbols. N_p pilot symbols are placed at the beginning of each subframe, and N_s data symbols are placed later. Postcoding weight is cyclically updated at reception of pilot symbols. The multiuser MIMO postcoding weight $\mathbf{W}^{(n)} \in \mathbb{C}^{N_\mathrm{r}\times N_\mathrm{d}}$ in the n-th subframe is expressed as

$$\mathbf{W}^{(n)} = \begin{bmatrix}\mathbf{w}_1^{(n)} & \mathbf{w}_2^{(n)} & \cdots & \mathbf{w}_{N_\mathrm{d}}^{(n)}\end{bmatrix}, \tag{1}$$

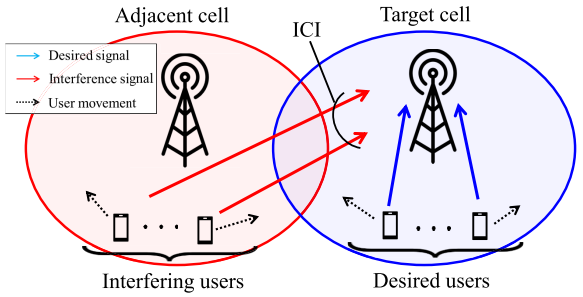

(a) System model.

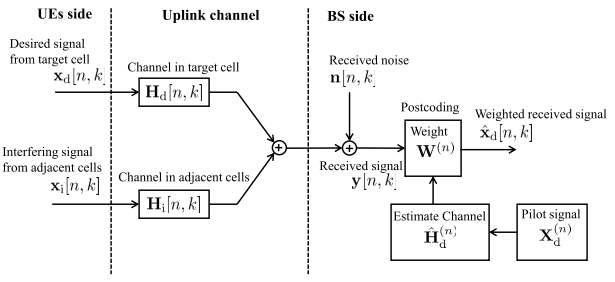

(b) The flow of a postcoding process.

FIGURE 1. System model and the flow of a postcoding.

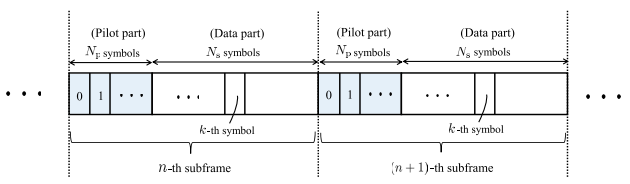

FIGURE 2. Frame structure.

where $\mathbf{w}_l^{(n)} = [w_{1l}^{(n)}, w_{2l}^{(n)}, \ldots, w_{N_r l}^{(n)}]^T \in \mathbb{C}^{N_r \times 1}$ is the postcoding weight vector in the n-th subframe for the l-th desired user. The received signal vector of the k-th symbol in the n-th subframe $\mathbf{y}[n,k] \in \mathbb{C}^{N_r \times 1}$ is represented as

$$\mathbf{y}[n,k] = \mathbf{H}_d[n,k]\mathbf{x}_d[n,k] + \mathbf{H}_i[n,k]\mathbf{x}_i[n,k] + \mathbf{n}[n,k] \quad k = 0,1,\ldots,N_p+N_s-1 \text{ and } n = 0,1,\ldots \tag{2}$$

where $\mathbf{x}_d = [x_{d1}, x_{d2}, \ldots, x_{dN_d}]^T \in \mathbb{C}^{N_d \times 1}$ is the transmission signal vector from desired users, and $\mathbf{x}_i = [x_{i1}, x_{i2}, \ldots, x_{iN_i}]^T \in \mathbb{C}^{N_i \times 1}$ is the transmission signal vector from interfering users. Transmission signal power of desired users and interfering users are ρ_d^2 and ρ_i^2. $\mathbf{n} \in \mathbb{C}^{N_r \times 1}$ is additive white Gaussian noise (AWGN) vector whose each component is modeled as a zero-mean complex Gaussian random variable with variance of σ_n^2. $\mathbf{H}_d = [\mathbf{h}_{d1}, \mathbf{h}_{d2}, \ldots, \mathbf{h}_{dN_d}] \in \mathbb{C}^{N_r \times N_d}$ and $\mathbf{H}_i = [\mathbf{h}_{i1}, \mathbf{h}_{i2}, \ldots, \mathbf{h}_{iN_i}] \in \mathbb{C}^{N_r \times N_i}$ are uplink channel matrices between desired users and BS antennas and between interfering users and BS antennas, respectively. $\mathbf{h}_{dl} = [h_{d1l}, h_{d2l} \ldots, h_{dN_r l}]^T \in \mathbb{C}^{N_r \times 1}$ and $\mathbf{h}_{im} = [h_{i1m}, h_{i2m} \ldots, h_{iN_r m}]^T \in \mathbb{C}^{N_r \times 1}$ represent channel vectors for the l-th desired user and for the m-th interfering user. We define the known pilot signal matrix from the desired users $\mathbf{X}_d^{(n)} \in \mathbb{C}^{N_d \times N_p}$, the unknown pilot signal matrix from the interfering users $\mathbf{X}_i^{(n)} \in \mathbb{C}^{N_i \times N_p}$, and the received pilot signal matrix $\mathbf{Y}^{(n)} \in \mathbb{C}^{N_r \times N_p}$ in the n-th subframe as

$$\mathbf{X}_d^{(n)} = \left[\, \mathbf{x}_d[n,0],\ \mathbf{x}_d[n,1],\ \ldots,\ \mathbf{x}_d[n,N_p-1] \right], \tag{3}$$

$$\mathbf{X}_i^{(n)} = \left[\, \mathbf{x}_i[n,0],\ \mathbf{x}_i[n,1],\ \ldots,\ \mathbf{x}_i[n,N_p-1] \right], \tag{4}$$

$$\mathbf{Y}^{(n)} = \left[\, \mathbf{y}[n,0],\ \mathbf{y}[n,1],\ \ldots,\ \mathbf{y}[n,N_p-1] \right]. \tag{5}$$

Here, we assume that the pilot symbol duration $N_p T_s$ is sufficiently smaller than channel coherence time T_c, where T_s is symbol duration. This means that the channel matrices $\mathbf{H}_d[n,k]$ and $\mathbf{H}_i[n,k]$ are time-varying but they remain constant matrix $\mathbf{H}_d^{(n)} \in \mathbb{C}^{N_r \times N_d}$ and $\mathbf{H}_i^{(n)} \in \mathbb{C}^{N_r \times N_i}$ over a short period of time. Therefore, it follows that

$$\mathbf{H}_d[n,0] = \mathbf{H}_d[n,1] = \cdots = \mathbf{H}_d[n,N_p-1] \triangleq \mathbf{H}_d^{(n)} \tag{6}$$

$$\mathbf{H}_i[n,0] = \mathbf{H}_i[n,1] = \cdots = \mathbf{H}_i[n,N_p-1] \triangleq \mathbf{H}_i^{(n)}. \tag{7}$$

Based on this assumption, the received signal matrix $\mathbf{Y}^{(n)}$ can be expressed as

$$\mathbf{Y}^{(n)} = \mathbf{H}_d^{(n)}\mathbf{X}_d^{(n)} + \mathbf{H}_i^{(n)}\mathbf{X}_i^{(n)} + \mathbf{N}^{(n)}. \tag{8}$$

From (8), the channel matrix in the target cell $\mathbf{H}_d^{(n)}$ can be estimated using known pilot signal matrix $\mathbf{X}_d^{(n)}$. Note that we cannot estimate the channel matrix in the adjacent cells $\mathbf{H}_i^{(n)}$ since the pilot signal matrix $\mathbf{X}_i^{(n)}$ from the interfering users is unknown. Estimate channel matrix $\hat{\mathbf{H}}_d^{(n)} \in \mathbb{C}^{N_r \times N_d}$ in least square (LS) manner [25] is given as

$$\begin{aligned}\hat{\mathbf{H}}_d^{(n)} &= \arg\min_{\mathbf{H}_d^{(n)}} \left\| \mathbf{Y}^{(n)} - \mathbf{H}_d^{(n)}\mathbf{X}_d^{(n)} \right\|_F^2 \\ &= \mathbf{Y}^{(n)}\mathbf{X}_d^{(n)\dagger} \\ &= \mathbf{H}_d^{(n)} + \underbrace{\mathbf{H}_i^{(n)}\mathbf{X}_i^{(n)}\mathbf{X}_d^{(n)\dagger} + \mathbf{N}^{(n)}\mathbf{X}_d^{(n)\dagger}}_{\text{Pilot contamination of ICI and AWGN}},\end{aligned} \tag{9}$$

where $\mathbf{X}_d^{(n)\dagger}$ means the pseudo-inverse matrix of $\mathbf{X}_d^{(n)}$. In (9), the second and third terms are pilot contamination by ICI and AWGN, which adversely affect the channel estimation accuracy. Besides, the channel estimation accuracy generally degrades in the latter of the subframe since the estimated channel $\hat{\mathbf{H}}_d^{(n)}$ is calculated at the beginning of the subframe. As shown in Fig. 1b, BS designs the postcoding weight $\mathbf{W}^{(n)}$ based on the estimated channel $\hat{\mathbf{H}}_d^{(n)}$. Then, using the postcoding weight $\mathbf{W}^{(n)}$, the transmission signal vector from desired users $\mathbf{x}_d[n,k]$ is estimated from the received signal vector $\mathbf{y}[n,k]$. The transmission signal from the l-th desired user of the k-th symbol in the n-th subframe $\hat{x}_{dl}[n,k]$ is estimated as

$$\begin{aligned}\hat{x}_{dl}[n,k] &= \mathbf{w}_l^{(n)H}\mathbf{y}[n,k] \\ &= \mathbf{w}_l^{(n)H}\mathbf{H}_d[n,k]\mathbf{x}_d[n,k] + \mathbf{w}_l^{(n)H}\mathbf{H}_i[n,k]\mathbf{x}_i[n,k] \\ &\quad + \mathbf{w}_l^{(n)H}\mathbf{n}[n,k] \\ &= \mathbf{w}_l^{(n)H}\mathbf{h}_{dl}[n,k]x_{dl}[n,k] \\ &\quad + \underbrace{\mathbf{w}_l^{(n)H}\mathbf{H}_{d\bar{l}}[n,k]\mathbf{x}_{d\bar{l}}[n,k]}_{\text{IUI}} \\ &\quad + \underbrace{\mathbf{w}_l^{(n)H}\mathbf{H}_i[n,k]\mathbf{x}_i[n,k]}_{\text{ICI}} + \underbrace{\mathbf{w}_l^{(n)H}\mathbf{n}[n,k]}_{\text{Received noise}}.\end{aligned} \tag{10}$$

In (10), the second and third terms represent IUI and ICI, respectively. These terms deteriorate the estimation accuracy of the desired signal. To suppress IUI and ICI, we should design the weight vector for the l-th desired user $\mathbf{w}_l^{(n)}$ under the null-steering conditions as

$$\mathbf{w}_l^{(n)H}\mathbf{H}_{d\bar{l}}[n,k] = \mathbf{O}_{1\times(N_d-1)} \tag{11}$$

$$\mathbf{w}_l^{(n)H}\mathbf{H}_i[n,k] = \mathbf{O}_{1\times N_i}. \tag{12}$$

However, IUI and ICI are not suppressed sufficiently due to the following three problems.

1) The channel of interfering users $\mathbf{H}_i^{(n)}$ cannot be estimated because pilot signal from interfering users are unknown.
2) The accuracy of the estimated channel $\hat{\mathbf{H}}_d^{(n)}$ is degraded due to ICI in (9).
3) The weight vector $\mathbf{w}_l^{(n)}$ is outdated due to channel time-variation.

B. NULL-SPACE EXPANSION (NSE)

Holding past Q estimated channel matrices, the NSE weight vector in the n-th subframe for the l-th desired user $\mathbf{w}_l^{(n)}$ is derived to satisfy the following condition.

$$\mathbf{w}_l^{(n)H}\hat{\mathbf{h}}_{dl}^{(n)} = 1 \tag{13}$$

$$\mathbf{w}_l^{(n)H}\hat{\mathbf{H}}_{d\bar{l}}^{(n-q)} = \mathbf{O}_{1\times(N_d-1)} \quad \text{for } q = 0,1,\ldots,Q-1 \text{ and } l = 1,2,\ldots,N_d \tag{14}$$

(13) denotes the condition of beamforming to the l-th desired user. (14) denotes the condition of null-steering to desired users except for the l-th desired user in order to suppress IUI. Concatenating all weight vectors constructs the NSE weight matrix $\mathbf{W}_{\mathrm{NSE}}^{(n)} = \left[\mathbf{w}_1^{(n)} \cdots \mathbf{w}_l^{(n)} \cdots \mathbf{w}_{N_\mathrm{d}}^{(n)}\right] \in \mathbb{C}^{N_\mathrm{r} \times N_\mathrm{d}}$. In (14), we see that the NSE weight vector $\mathbf{w}_l^{(n)}$ is orthogonal to the channel vectors except for l-th desired user at past time instants $\{n-1,\ n-2,\ \ldots,\ n-Q+1\}$ as well as the latest time instant n. Here, to explain the advantage of the NSE scheme, we define "null-space" as a vector subspace to be orthogonalized to the weight vector. For example, when $Q = 2$ and $N_\mathrm{d} = 2$, null-space obtained by the NSE weight vector for the 1st desired user $\mathbf{w}_1^{(n)}$ is shown in Fig. 3. Its null-space dimension is 2 since weight vector $\mathbf{w}_1^{(n)}$ is designed to be orthogonal to the estimated channel vectors $\hat{\mathbf{h}}_{\mathrm{d}2}^{(n)}$ and $\hat{\mathbf{h}}_{\mathrm{d}2}^{(n-1)}$. In general, null-space dimension obtained by the NSE weight vector $\mathbf{w}_l^{(n)}$ is $Q(N_\mathrm{d}-1)$. If the time-varying interference channel vector exists in null-space, IUI can be completely suppressed because of the orthogonality between the time-varying interference channel vector and the NSE weight vector. Spanning a high-dimensional null-space is effective to IUI suppression since the time-varying interference channel vector likely moves in that space [12], [21]. In particular, the NSE scheme has the property of the orthogonality between the NSE weight vector and the predicted channel vectors by AR model [9]. The predicted channel vector by AR model of order Q for the k-th desired user in the $(n+1)$-th subframe is given as

$$\hat{\mathbf{h}}_{\mathrm{d}k}^{(n+1)} = \sum_{q=0}^{Q-1} a_{k,q} \hat{\mathbf{h}}_{\mathrm{d}k}^{(n-q)}, \tag{15}$$

where $a_{k,q}$ represent AR coefficients determined by Yule-Walker equation [9]. We obtain the following equation by extracting only the channel vector of k-th desired user from the NSE condition (14).

$$\mathbf{w}_l^{(n)H} \hat{\mathbf{h}}_{\mathrm{d}k}^{(n-q)} = 0 \quad \text{for } q = 0, 1, \ldots, Q-1 \text{ and } k \neq l. \tag{16}$$

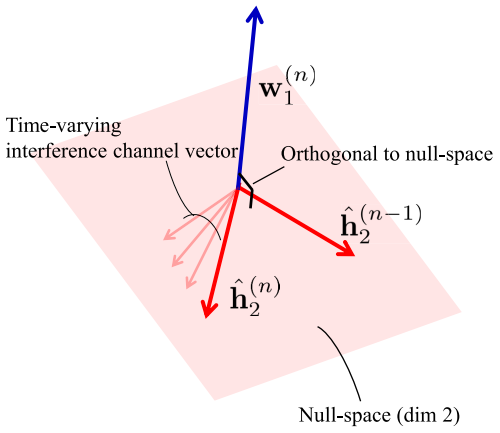

FIGURE 3. Null-space when $Q = 2$ and $N_\mathrm{d} = 2$.

From (15) and (16), we obtain

$$\mathbf{w}_l^{(n)H} \hat{\mathbf{h}}_{\mathrm{d}k}^{(n+1)} = \sum_{q=0}^{Q-1} a_{k,q} \mathbf{w}_l^{(n)H} \hat{\mathbf{h}}_{\mathrm{d}k}^{(n-q)} = 0, \quad \text{for } k \neq l. \tag{17}$$

In (17), the NSE weight vector $\mathbf{w}_l^{(n)}$ is orthogonal to the predicted channel vector based on AR model $\hat{\mathbf{h}}_{\mathrm{d}k}^{(n+1)}$, whatever the value of AR coefficients $a_{k,q}$ are. Therefore, by designing the NSE weight under the condition (14), we expect high IUI suppression capability even in time-varying environments. However, the NSE weight vector obtained by (14) cannot properly suppress IUI due to channel estimation error in (9). It also does not suppress unknown interference such as ICI at all since it cannot nullify interfering users in adjacent cells.

C. SAMPLE MATRIX INVERSION (SMI)

SMI algorithm can suppress an unknown interference based on an MMSE manner [15]. Compared to other interference suppression algorithms such as LMS and RLS, SMI has higher computational complexity due to the matrix inversion operation but has excellent interference suppression performance [26]. The weight of MMSE is obtained by solving the following optimization problem.

$$\min_{\mathbf{W}} \mathrm{E}\left[\left\|\mathbf{x}_\mathrm{d} - \mathbf{W}^H \mathbf{y}\right\|_\mathrm{F}^2\right] \tag{18}$$

The SMI weight in the n-th subframe is derived as

$$\begin{aligned} \mathbf{W}_{\mathrm{SMI}}^{(n)} &= \left\{\mathbf{R}_{\mathbf{yy}}^{(n)}\right\}^{-1} \mathbf{R}_{\mathbf{yx_d}}^{(n)} \\ \mathbf{R}_{\mathbf{yy}}^{(n)} &= \frac{1}{N_\mathrm{p}} \mathbf{Y}^{(n)} \mathbf{Y}^{(n)H} \\ \mathbf{R}_{\mathbf{yx_d}}^{(n)} &= \frac{1}{N_\mathrm{p}} \mathbf{Y}^{(n)} \mathbf{X}_\mathrm{d}^{(n)H} \end{aligned} \tag{19}$$

where $\mathbf{R}_{\mathbf{yy}}^{(n)}$ and $\mathbf{R}_{\mathbf{yx_d}}^{(n)}$ are the sample auto-correlation matrix of the received signal and the sample cross-correlation matrix between the received signal and the reference signal, respectively. The SMI algorithm works to suppress interference signals other than reference signals transmitted by desired users. Therefore, not only IUI suppression but also ICI suppression is attained. However, the performance of the SMI algorithm deteriorates with time in time-varying channel environments since the weight $\mathbf{W}_{\mathrm{SMI}}^{(n)}$ is calculated by using pilot symbols as reference signals at the beginning of the n-th subframe.

III. PROPOSED SCHEME

In the proposed scheme, the past Q pilot symbols are utilized as with the conventional NSE scheme. We define the extended received pilot signal matrix $\mathbf{Y}_\mathrm{e}^{(n)} \in \mathbb{C}^{N_\mathrm{r} \times QN_\mathrm{p}}$ and the extended pilot signal matrix $\mathbf{X}_\mathrm{de} \in \mathbb{C}^{N_\mathrm{d} \times QN_\mathrm{p}}$, which stack the past QN_p symbols in the column direction as

$$\mathbf{Y}_\mathrm{e}^{(n)} = \left[\mathbf{Y}^{(n)}\ \mathbf{Y}^{(n-1)} \cdots \mathbf{Y}^{(n-Q+1)}\right] \tag{20}$$

$$\mathbf{X}_\mathrm{de}^{(n)} = \left[\mathbf{X}_\mathrm{d}^{(n)}\ \mathbf{X}_\mathrm{d}^{(n-1)} \cdots \mathbf{X}_\mathrm{d}^{(n-Q+1)}\right]. \tag{21}$$

From (20), (21), the proposed weight can be derived by solving the optimization problem as

$$\mathbf{W}_{\text{prop}}^{(n)} = \arg\min_{\mathbf{W}^{(n)}} \left\| \mathbf{X}_{\text{de}}^{(n)} - \mathbf{W}^{(n)H} \mathbf{Y}_{\text{e}}^{(n)} \right\|_{\text{F}}^{2}. \tag{22}$$

To derive the above weight matrix $\mathbf{W}_{\text{prop}}^{(n)}$, we define the objective function J to be minimized. It can be transformed as

$$\begin{aligned} J &\triangleq \left\| \mathbf{X}_{\text{de}}^{(n)} - \mathbf{W}^{(n)H} \mathbf{Y}_{\text{e}}^{(n)} \right\|_{\text{F}}^{2} \\ &= \text{tr}\left\{ \left(\mathbf{X}_{\text{de}}^{(n)} - \mathbf{W}^{(n)H} \mathbf{Y}_{\text{e}}^{(n)} \right) \left(\mathbf{X}_{\text{de}}^{(n)} - \mathbf{W}^{(n)H} \mathbf{Y}_{\text{e}}^{(n)} \right)^{H} \right\} \\ &= \text{tr}\left(\mathbf{W}^{(n)H} \mathbf{Y}_{\text{e}}^{(n)} \mathbf{Y}_{\text{e}}^{(n)H} \mathbf{W}^{(n)} \right) - \text{tr}\left(\mathbf{W}^{(n)H} \mathbf{Y}_{\text{e}}^{(n)} \mathbf{X}_{\text{de}}^{(n)H} \right) \\ &\quad - \text{tr}\left(\mathbf{X}_{\text{de}}^{(n)} \mathbf{Y}_{\text{e}}^{(n)H} \mathbf{W}^{(n)} \right) + \text{tr}\left(\mathbf{X}_{\text{de}}^{(n)} \mathbf{X}_{\text{de}}^{(n)H} \right). \end{aligned} \tag{23}$$

To minimize objective function J, we find the optimal solution by taking the partial derivative of J with respect to $\mathbf{W}^{(n)}$ and setting to zero; we have

$$\frac{\partial J}{\partial \mathbf{W}^{(n)*}} = \mathbf{Y}_{\text{e}}^{(n)} \mathbf{Y}_{\text{e}}^{(n)H} \mathbf{W}_{\text{prop}}^{(n)} - \mathbf{Y}_{\text{e}}^{(n)} \mathbf{X}_{\text{de}}^{(n)H} = \mathbf{O}_{N_{\text{r}} \times N_{\text{d}}}. \tag{24}$$

From (20), (21), and (24), we can obtain the proposed weight matrix as

$$\begin{aligned} \mathbf{W}_{\text{prop}}^{(n)} &= \left(\mathbf{Y}_{\text{e}}^{(n)} \mathbf{Y}_{\text{e}}^{(n)H} \right)^{-1} \mathbf{Y}_{\text{e}}^{(n)} \mathbf{X}_{\text{de}}^{(n)H} \qquad (25) \\ &= \left\{ \sum_{q=0}^{Q-1} \mathbf{Y}^{(n-q)} \mathbf{Y}^{(n-q)H} \right\}^{-1} \sum_{q=0}^{Q-1} \mathbf{Y}^{(n-q)} \mathbf{X}_{\text{d}}^{(n-q)H} \\ &= \left\{ \sum_{q=0}^{Q-1} \mathbf{R}_{\mathbf{yy}}^{(n-q)} \right\}^{-1} \sum_{q=0}^{Q-1} \mathbf{R}_{\mathbf{yx_d}}^{(n-q)}. \qquad (26) \end{aligned}$$

The weight matrix $\mathbf{W}_{\text{prop}}^{(n)}$ satisfy the following properties when $\mathbf{N}^{(n)} = \mathbf{O}_{N_{\text{r}} \times N_{\text{p}}}$ and $(N_{\text{d}} + N_{\text{i}}) \leqq N_{\text{p}}$ in (8).

$$\mathbf{W}_{\text{prop}}^{(n)H} \mathbf{H}_{\text{d}}^{(n-q)} = \mathbf{I}_{N_{\text{d}}} \tag{27}$$

$$\mathbf{W}_{\text{prop}}^{(n)H} \mathbf{H}_{\text{i}}^{(n-q)} = \mathbf{O}_{N_{\text{d}} \times N_{\text{i}}} \quad \text{for } q = 0,\ 1,\ \ldots,\ Q-1. \tag{28}$$

We provide proof of properties (27) and (28) in Appendix. Extracting only the proposed weight vector of l-th desired user $\mathbf{w}_{l}^{(n)}$ from (27) and (28), we obtain

$$\mathbf{w}_{l}^{(n)H} \mathbf{h}_{\text{d}l}^{(n-q)} = 1 \tag{29}$$

$$\mathbf{w}_{l}^{(n)H} \mathbf{H}_{\text{d}\bar{l}}^{(n-q)} = \mathbf{O}_{1 \times (N_{\text{d}}-1)} \tag{30}$$

$$\mathbf{w}_{l}^{(n)H} \mathbf{H}_{\text{i}}^{(n-q)} = \mathbf{O}_{1 \times N_{\text{i}}} \quad \text{for } q = 0, 1, \ldots, Q-1 \text{ and } l = 1, 2, \ldots, N_{\text{d}}. \tag{31}$$

(30) indicates null-steering to desired users except for the l-th desired user at the past Q time instants, which leads to IUI suppression. (31) indicates null-steering to all interfering users at the past Q time instants, which leads to ICI suppression. Although the conventional NSE scheme attempts to suppress only IUI in (14), the proposed scheme can suppress ICI as well as IUI in (30), (31). As a result, null-space is expanded to the $Q(N_{\text{d}}+N_{\text{i}}-1)$ dimension. IUI suppression performance of the conventional NSE scheme degrades due to the channel estimation error caused by pilot contamination in (9), but the proposed scheme can mitigate such impact since it uses received pilot sequences themselves and can suppress both IUI and ICI at the same time. Therefore, it has superior IUI and ICI suppression capabilities for future time-varying channels compared to the conventional NSE scheme.

From (26), the proposed weight can be designed with relatively small computational complexity operations less than the conventional NSE. Summation of the correlation matrices $\sum_{q=0}^{Q-1} \mathbf{R}_{\mathbf{yy}}^{(n-q)}$ and $\sum_{q=0}^{Q-1} \mathbf{R}_{\mathbf{yx_d}}^{(n-q)}$ in (26) do not enlarge these size, and thus the complexities of matrix inversion operation cannot be increased. Table 2 summarizes estimated computation complexities in terms of the number of complex multiplications. In this table, p is the total consumed DoFs by designing the NSE weight in (13), (14). Therefore, p is given as $p = Q(N_{\text{d}} - 1) + 1$, where $Q(N_{\text{d}} - 1)$ indicates the expanded null-space dimension in the conventional NSE scheme. Detailed values are also exemplified with parameters when $N_{\text{r}} = 100, N_{\text{d}} = 8, N_{\text{p}} = 16$ and $Q = 6$. In this case, complexity required for the proposed scheme is reduced by 16.8 % compared with that for the conventional NSE. Its realistic impact especially on the latency performance could be dependent on the hardware resource. Although the supposed scenario is the uplink where some processing delay is acceptable, its detailed applicability can be optimized by coordinating the pilot transmission interval, the number of past pilot sequences Q, and other related parameters.

TABLE 2. Computation complexity.

Scheme	Values (example at $N_{\text{r}}=100$, $N_{\text{d}}=8$, $N_{\text{p}}=16$ and $Q=6$)
SMI	$N_{\text{p}}N_{\text{r}}^2 + N_{\text{p}}N_{\text{d}}N_{\text{r}} + N_{\text{r}}^2N_{\text{d}} + (N_{\text{r}}^3 + 3N_{\text{r}}^2 - N_{\text{r}})/3$ (596,100)
NSE	$p^2N_{\text{d}}N_{\text{r}} + p^2N_{\text{d}} + pN_{\text{d}}N_{\text{r}} + N_{\text{d}}(p^3 + 3p^2 - p)/3$ where $p = Q(N_{\text{d}} - 1) + 1$ (1,755,088)
Proposed	$QN_{\text{p}}N_{\text{r}}^2 + QN_{\text{p}}N_{\text{d}}N_{\text{r}} + N_{\text{r}}^2N_{\text{d}} + (N_{\text{r}}^3 + 3N_{\text{r}}^2 - N_{\text{r}})/3$ (1,460,100)

IV. NUMERICAL RESULTS

A. SIMULATION PARAMETERS

Simulation parameters are listed in Table 3. In the simulation, the carrier frequency is set to 28 GHz which is licensed for the 5G system. We assume a small cell scenario, as shown in Fig. 4. The height of BS is 10 m, and the radius of the cell is 20 m. BS has 10 × 10 elements square uniform planar array (UPA) with half-wavelength spacing. As shown in Fig. 4, 8 desired users and 2 interfering users are randomly distributed in the desired area and interfering areas, respectively. All users move random directions at velocity v [km/h]. We assume single-carrier narrow band transmission and Rayleigh and Rician fading channel environments [27].

TABLE 3. Simulation parameters.

Parameter	Values
Frequency	28 GHz
Cell	Sector 120°, Radius 20 m
Number of BS antennas N_r	100 (10 × 10 elements square UPA with half-wavelength spacing)
Number of desired users N_d	8
Number of interfering users N_i	2
Number of data symbols N_s	84 symbols
Number of pilot symbols N_p	16 symbols
Symbol duration T_s	8.33 μs
Pilot transmission period	100 symbols (0.833 ms)
CSI estimation	Least square
Channel model	(x) i.i.d Rayleigh, (y) Rician with spatial correlation ($K = 10$)
AoA distribution	Gaussian distribution (Azimuth) Laplacian distribution (Elevation) with 5° AS [30]
BS antenna pattern	Directional antenna with 65° HPBW (Vertical/Horizontal) [30]
User velocity v	10 km/h ($f_\mathrm{D}T_\mathrm{s} = 2.16\times10^{-3}$)
input SIR $\rho_\mathrm{d}^2/\rho_\mathrm{i}^2$	0 dB
input SNR $\rho_\mathrm{d}^2/\sigma_\mathrm{n}^2$	30 dB

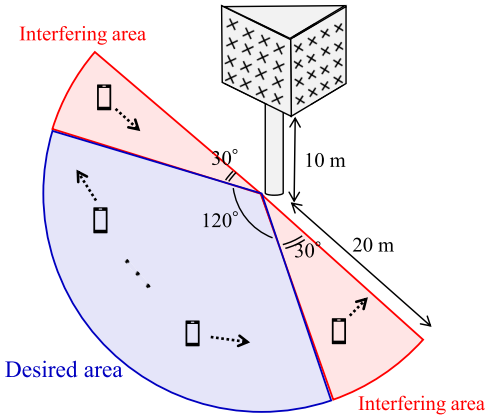

FIGURE 4. Simulated cell configuration.

The channel vectors of Rician fading for the l-th desired user $\mathbf{h}_{\mathrm{d}l}$ and the m-th interfering user $\mathbf{h}_{\mathrm{i}m}$ are modeled as

$$\mathbf{h}_{\mathrm{d}l} = \sqrt{\frac{K}{K+1}}\mathbf{h}_{\mathrm{d}l,\mathrm{LoS}} + \sqrt{\frac{1}{K+1}}\mathbf{h}_{\mathrm{d}l,\mathrm{NLoS}} \quad l = 1, 2, \ldots, N_\mathrm{d} \tag{32}$$

$$\mathbf{h}_{\mathrm{i}m} = \sqrt{\frac{K}{K+1}}\mathbf{h}_{\mathrm{i}m,\mathrm{LoS}} + \sqrt{\frac{1}{K+1}}\mathbf{h}_{\mathrm{i}m,\mathrm{NLoS}} \quad m = 1, 2, \ldots, N_\mathrm{i} \tag{33}$$

where $\mathbf{h}_{\mathrm{d}l,\mathrm{LoS}}$ and $\mathbf{h}_{\mathrm{i}m,\mathrm{LoS}}$ are the line-of-sight (LoS) signal components determined by the positional relation between users and BS, and $\mathbf{h}_{\mathrm{d}l,\mathrm{NLoS}}$ and $\mathbf{h}_{\mathrm{i}m,\mathrm{NLoS}}$ are the non-line-of-sight (NLoS) signal components from the scatterers around each user. The parameter K is the Rician K-factor, defined as the ratio between the LoS path gain to the NLoS path gain. To consider the spatial correlation between BS antenna elements, we generate correlated channel vectors $\mathbf{h}_{\mathrm{d}l,\mathrm{NLoS}}$ and $\mathbf{h}_{\mathrm{i}m,\mathrm{NLoS}}$ by Kronecker model [28].

$$\mathbf{h}_{\mathrm{d}l,\mathrm{NLoS}} = \mathbf{R}_{\mathrm{d}l}^{\frac{1}{2}}\mathbf{h}_{\mathrm{d}l,\mathrm{iid}} \quad l = 1, 2, \ldots, N_\mathrm{d} \tag{34}$$

$$\mathbf{h}_{\mathrm{i}m,\mathrm{NLoS}} = \mathbf{R}_{\mathrm{i}m}^{\frac{1}{2}}\mathbf{h}_{\mathrm{i}m,\mathrm{iid}} \quad m = 1, 2, \ldots, N_\mathrm{i} \tag{35}$$

where each element of $\mathbf{h}_{\mathrm{d}l,\mathrm{iid}}$ and $\mathbf{h}_{\mathrm{i}m,\mathrm{iid}}$ are independent and identically distributed (i.i.d.) Rayleigh fading channel coefficient generated by the Jakes' model [29], and $\mathbf{R}_{\mathrm{d}l} \in \mathbb{C}^{N_\mathrm{r}\times N_\mathrm{r}}$ and $\mathbf{R}_{\mathrm{i}m} \in \mathbb{C}^{N_\mathrm{r}\times N_\mathrm{r}}$ are spatial correlation matrices at BS side. In the simulation, we compare the following two types of channel environments.

(x) i.i.d Rayleigh fading channel
(y) Rician fading channel with spatial correlation

In (x), we do not consider the LoS component and the spatial correlation, therefore $K = 0$ ($-\infty$ dB), $\mathbf{R}_{\mathrm{d}l} = \mathbf{I}_{N_\mathrm{r}}$ and $\mathbf{R}_{\mathrm{i}m} = \mathbf{I}_{N_\mathrm{r}}$ in (32)-(35). In (y), we assume Rician fading channel with $K = 10$ considering spatial correlation and the LoS as well as the NLoS components. The spatial correlation matrices $\mathbf{R}_{\mathrm{d}l}$ and $\mathbf{R}_{\mathrm{i}m}$ are calculated by Gaussian and Laplacian angle of arrival (AoA) distributions with 5° angular spread (AS) and directional antenna pattern with 65° half-power bandwidth (HPBW) [30].

The evaluation metric is output SINR defined as

$$\mathrm{SINR}[n,k] = \frac{P_\mathrm{d}[n,k]}{P_\mathrm{i}[n,k] + \sigma_\mathrm{n}^2\|\mathbf{W}^{(n)}\|_\mathrm{F}^2} \tag{36}$$

$$P_\mathrm{d}[n,k] = \frac{\rho_\mathrm{d}^2}{N_\mathrm{d}}\sum_{l=1}^{N_\mathrm{d}}\mathrm{E}\left[\left|\left(\mathbf{W}^{(n)H}\mathbf{H}_\mathrm{d}[n,k]\right)_{ll}\right|^2\right] \tag{37}$$

$$P_\mathrm{i}[n,k] = \frac{\rho_\mathrm{d}^2}{N_\mathrm{d}}\sum_{l\neq m}\mathrm{E}\left[\left|\left(\mathbf{W}^{(n)H}\mathbf{H}_\mathrm{d}[n,k]\right)_{lm}\right|^2\right] + \frac{\rho_\mathrm{i}^2}{N_\mathrm{d}}\mathrm{E}\left[\left\|\mathbf{W}^{(n)H}\mathbf{H}_\mathrm{i}[n,k]\right\|_\mathrm{F}^2\right] \tag{38}$$

where $P_\mathrm{d}[n,k]$ and $P_\mathrm{i}[n,k]$ are desired and interference signal power in array output per one desired user. In (36)–(38), we approximate the expectation $\mathrm{E}[\cdot]$ by the average operation of 100 repeated trials in the time-varying channel realizations randomly generated.

The following five postcoding schemes are compared.

(a) Conventional Sample matrix inversion (SMI)
(b-1) Channel prediction by Autoregressive model (AR) [9]
(b-2) Channel prediction by first-order Taylor expansion model (FIT) [10]
(c) Conventional Null-Space Expansion scheme (NSE)
(d) Proposed scheme (Prop)

The SINR is calculated at every symbol reception timing as shown in Fig. 5. In the conventional SMI algorithm (a), the postcoding weight is designed by only one received pilot

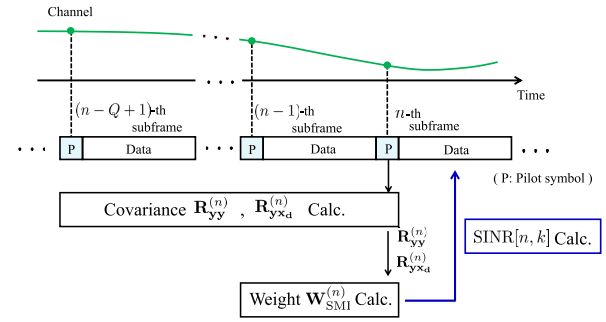

(a) Sample Matrix Inversion (SMI).

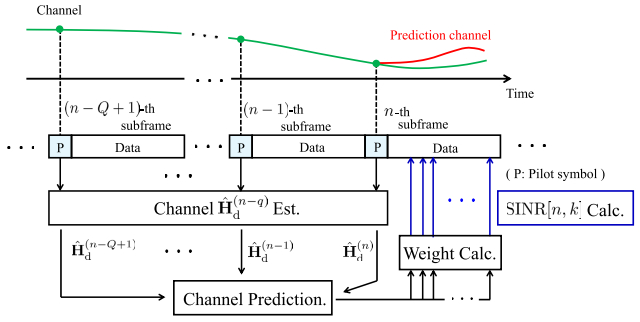

(b) Channel prediction scheme (AR, FIT).

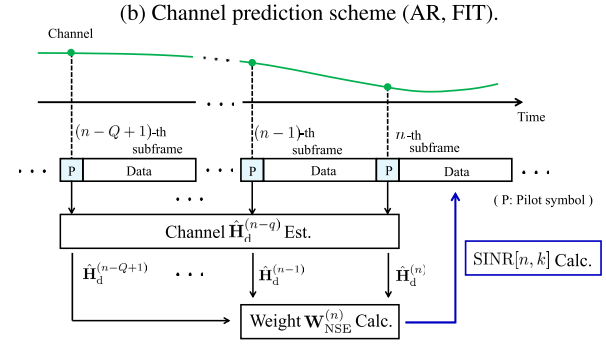

(c) Null-Space Expansion scheme (NSE).

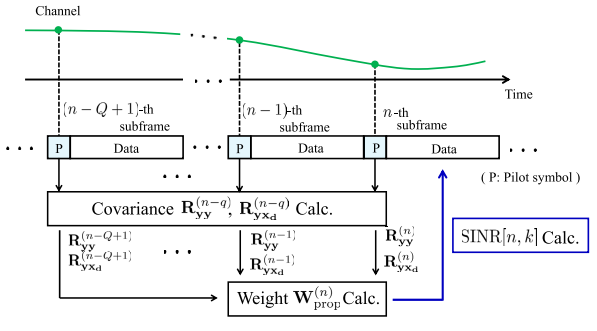

(d) Proposed scheme (Prop).

FIGURE 5. SINR calculation flow in time-varying channel.

sequence at the beginning of the subframe. In the conventional NSE scheme (c), the postcoding weight is designed by past Q estimated channels. In the proposed scheme (d), the postcoding weight is designed by past Q received pilot sequences. In the channel prediction scheme (b-1) and (b-2), we predict future channels in one subframe duration using past Q estimated channels. Then, based on the predicted channels, we design Zero-Forcing weight [31], which is commonly used as a postcoding weight in MIMO system, at every symbol reception timing.

We perform the least square (LS) channel estimation scheme. The channel estimation error is assumed to be caused by ICI, received noise, and channel-time variation. The transmission timing of the pilot symbol is every 100 symbols. Unless otherwise noted, the input SIR $\frac{\rho_\mathrm{d}^2}{\rho_\mathrm{i}^2}$ and input SNR $\frac{\rho_\mathrm{d}^2}{\sigma_\mathrm{n}^2}$ are 0 dB and 30 dB, respectively.

B. SIMULATION RESULTS

1) OUTPUT SINR WITH TIME TRANSIENT

Fig. 6 shows the transition of SINR for one subframe duration in Rayleigh and Rician fading channels when user velocity is $v = 10$ km/h and the number of past pilot sequences is $Q = 5, 6$. In this figure, SINR is relatively high just after 0 seconds since the weight calculation is performed at the time of 0 seconds. The SINR values decrease with time for each scheme. However, the proposed scheme keeps the SINR

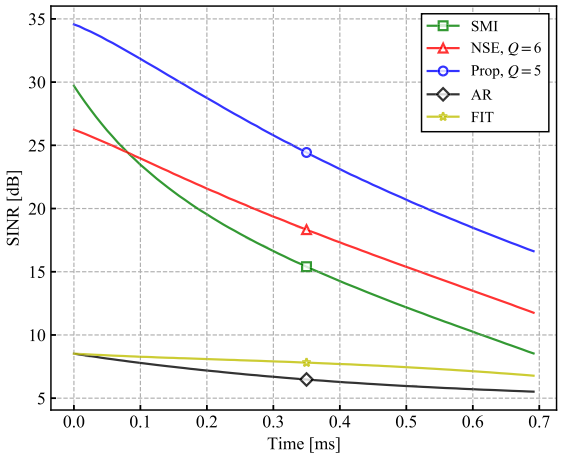

(a) Rayleigh fading channel.

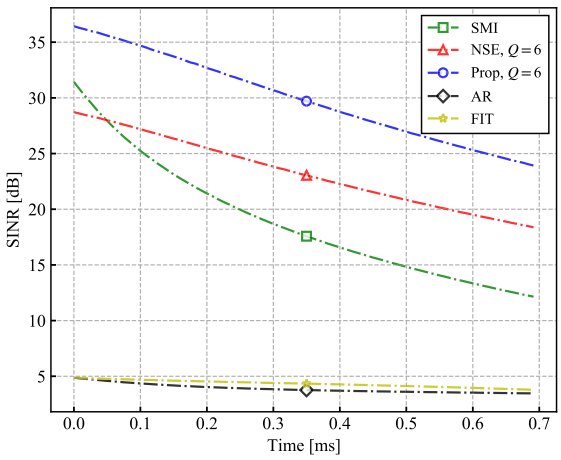

(b) Rician fading channel.

FIGURE 6. Transition of SINR with time progress ($v = 10$ km/h, SIR = 0 dB, SNR = 30 dB).

values higher than other schemes in both Rayleigh and Rician fading channels. On the other hand, the SINR performance of channel prediction schemes, AR and FIT, is low compared to the other schemes. This is because pilot contamination by ICI in (9) deteriorates the accuracy of channel estimation. It leads to difficulty with the appropriate future channel prediction.

2) OUTPUT SINR WITH THE NUMBER OF PAST PILOT SEQUENCES

Fig. 7 shows the time-averaged SINR, output interference power, and output desired power in one subframe versus the number of past pilot sequences Q when user velocity $v = 10$ km/h. The powers are normalized in the condition that the transmission signal power of desired users ρ_{d}^2 is to be 1, and Frobenius norm of the weight $\|\mathbf{W}^{(n)}\|_{\mathrm{F}}^2$ is also set to 1. In this figure, $Q = 1$ in the proposed scheme means the conventional SMI algorithm. In other cases, past Q pilot symbols are used to design postcoding weights. Fig. 7a shows the SINR versus the number of past pilot sequences Q. In Rayleigh fading channel, the maximum SINR of the NSE scheme is 17.7 dB at $Q = 6$, and that of the proposed scheme is 22.5 dB at $Q = 5$. In this case, the proposed scheme improves the SINR value by about 4.8 dB. In Rician fading channel, the maximum SINR of the NSE scheme is 22.4 dB at $Q = 6$, and that of the proposed scheme is 28.6 dB at $Q = 6$. In this case, SINR improvement provided by the proposed scheme is about 6.2 dB. As expressed in (14), the conventional NSE additionally nullifies only for the desired users. When $Q = 9$, the dimension of the null-space of the conventional NSE is $(8 - 1) \times 9 = 63$ since the number of desired users is 8. On the other hand, the proposed scheme nullifies not only for the desired user but also for the interfering user in the adjacent cells, as formulated in (30) and (31). The null-space dimension for the proposed scheme is $(10-1)\times 9 = 81$ since the number of total users, including interfering users, is 10. In both methods, the dimension of the null-space is a possible region since it is smaller than the DoFs of BS, $N_{\mathrm{r}} = 100$.

Fig. 7b shows the output interference power versus the number of past pilot sequences Q. We see that the output interference power is decreased as Q increases. As described in Section II-B, the interference suppression capability can be improved since the null-space is expanded with the increase of Q. In particular, the proposed scheme can significantly reduce the output interference power compared to the conventional NSE. This effectiveness is remarkable especially in the Rician fading channel. This notable advantage is derived from suppressing ICI, which could not be suppressed by the conventional NSE.

Fig. 7c shows the output desired power versus the number of past pilot sequences Q. We see that the increasing Q degrades the output desired signal power for both schemes. This is because expanding the null-space consumes the DoFs originally allocated to obtain the desired power gain. In particular, the severe deterioration of the output desired signal power is observed in the proposed scheme. Since the proposed scheme performs null-steering to both the desired users and the interfering users as shown in (30) and (31), it consumes more DoFs than the conventional NSE scheme, which nullifies only to the desired users in (14).

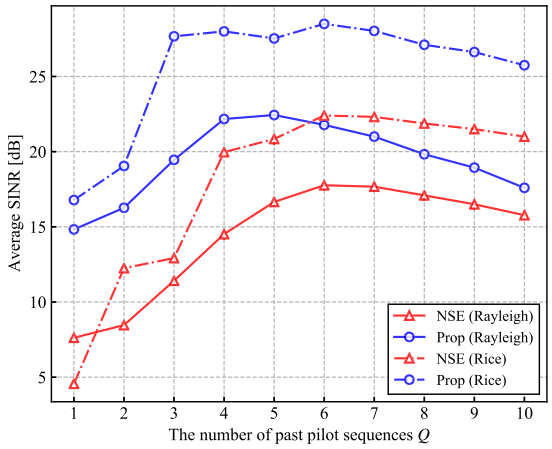

(a) Output SINR.

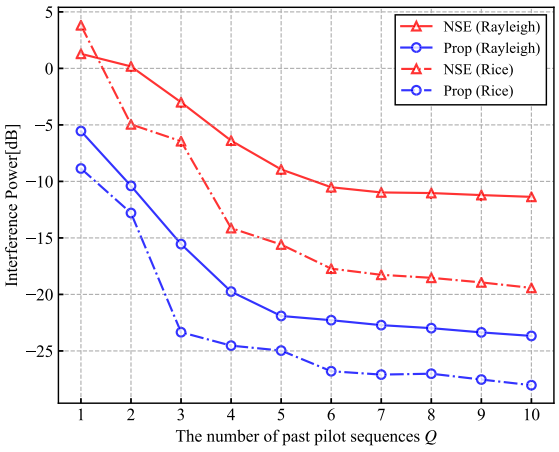

(b) Output interference power.

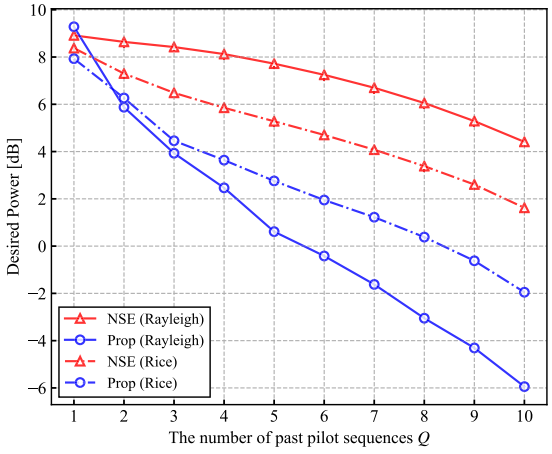

(c) Output desired power.

FIGURE 7. Time-averaged SINR, output desired power, and output interference power versus the number of past pilot sequences Q ($v = 10$ km/h, SIR = 0 dB, SNR = 30 dB).

As shown in Fig. 7a, the SINR increases as Q increases, but when Q exceeds a certain value, the SINR starts to decrease. The cause of the decreasing SINR can be seen in Fig. 7b and Fig. 7c. In Fig. 7b, the interference power decreases as Q increases, but when Q exceeds a certain value, the decreasing of the interference power is gradual. It indicates that there are no more interference channel vectors that are highly correlated with the expanded null-space. On the other hand, as shown in Fig. 7c, the desired signal power monotonically decreases as Q increases. Therefore, when Q exceeds a certain value, the adverse effects of the decrease in the desired signal power outweigh the benefits of the interference suppression. It then results in the reduction of output SINR.

3) OUTPUT SINR WITH MOVING SPEED

Fig. 8 shows the time-averaged SINR in one subframe versus user velocity v in Rayleigh and Rician fading channel environments. In all schemes, output SINR values decrease as the user velocity increases. This tendency can be discussed with the coherence time related to the moving velocity. The coherence time is defined as the range of time duration over which the channel temporal-correlation is above a definite value r_{th}. In Rayleigh fading channel, the channel coherence time is given as [32]

$$T_{\mathrm{c}} = \frac{J_0^{-1}(r_{\mathrm{th}})}{\pi f_{\mathrm{D}}}. \tag{39}$$

J_0 is the zeroth-order Bessel function of the first kind, and f_{D} is the maximum Doppler frequency given by $f_{\mathrm{D}} = v/\lambda$ where λ denotes the wavelength. As expressed above, the coherence time can be represented by the user velocity; it decreases as the user moves fast. In Rayleigh fading channel, the performance of the proposed scheme is better than the other schemes at lower velocity up to $v = 10$ km/h. When the user velocity is small, that is, in large coherence time, the null space expansion works effectively because time-varying interference channel vectors move in a limited subspace due to the high temporal correlation. At a high velocity above $v = 16$ km/h, the performance of the proposed scheme is less than the other schemes. On the other hand, in Rician fading channel, the performance of the proposed scheme is the best at all velocityies. The temporal-correlation in Rician fading channel is greater than that of Rayleigh environment thanks to the presence of the LOS component [33]. It also lengthens the practical coherence time in Rician fading channel, and hence the proposed scheme works well even in high mobility situations.

4) OUTPUT SINR WITH INPUT SIR

Fig. 9 plots the time-averaged SINR in one subframe versus input SIR when user velocity is $v = 10$ km/h and input SNR is 30 dB. The SINR performances of NSE, AR, and FIT are improved as the input SIR increases. This is because the pilot contamination impact in (9) is alleviated in the high SIR region; channel estimation accuracy is hence improved. In Rayleigh fading channel, the proposed scheme is superior to

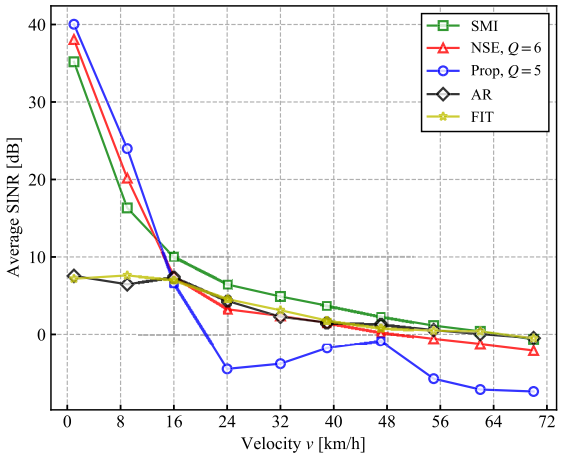

(a) Rayleigh fading chanel.

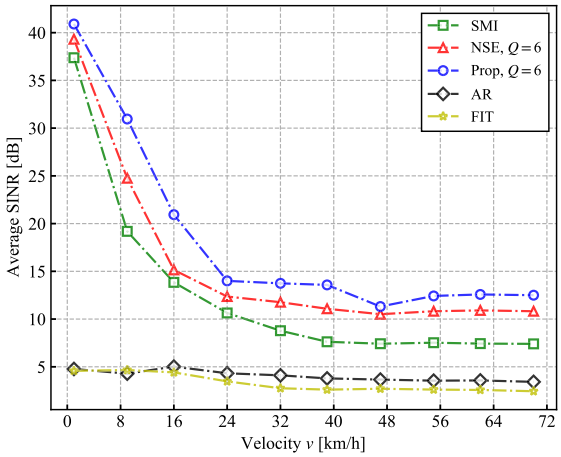

(b) Rician fading channel.

FIGURE 8. Time-averaged SINR in one subframe versus user velocity v (SIR = 0 dB, SNR = 30 dB).

the conventional schemes when input SIR is lower than about 10 dB since IUI suppression performance of the conventional NSE is hindered from imperfect CSI due to the unknown interference incoming with a higher power. In Rician fading channel, the performance of the proposed scheme is better than the conventional NSE when the SIR is lower than about 20 dB. Compared with Rayleigh fading channel, the input SIR region where the proposed scheme shows the best output SINR performance increases by about 10 dB.

5) OUTPUT SINR WITH INPUT SNR

Finally, Fig. 10 shows the time-averaged SINR in one subframe versus input SNR. User velocity is $v = 10$ km/h and input SIR is 0 dB. In Rayleigh fading channel, when input SNR is lower than about 15 dB, the performance of the proposed scheme is less than that of the conventional schemes. In such low SNR region, the interference suppression capability of the proposed scheme deteriorates since additional nulls cannot be steered properly to the past interference channels due to the noisy pilot signals. Nevertheless, the performance

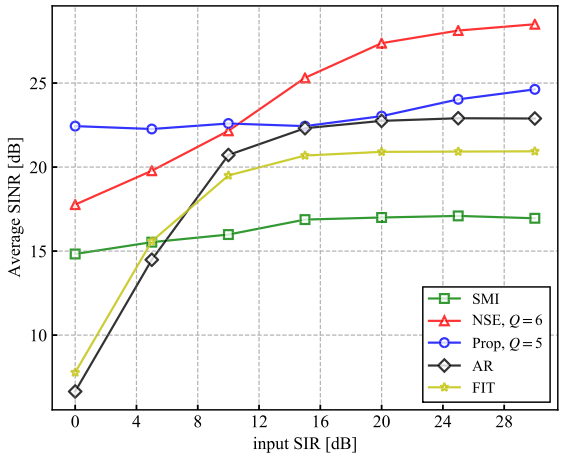

(a) Rayleigh fading channel.

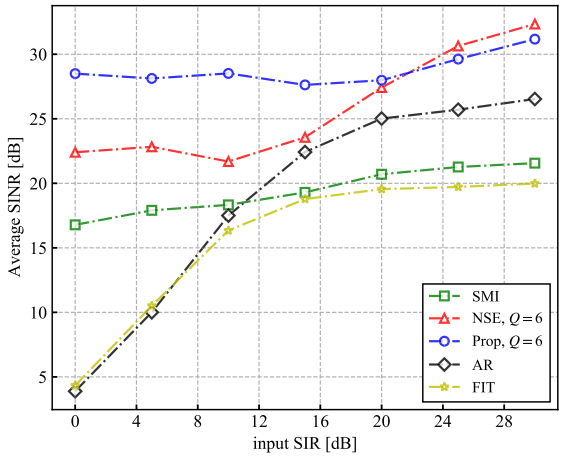

(b) Rician fading channel.

FIGURE 9. Time-averaged SINR per subframe versus input SIR (v = 10 km/h, SNR = 30 dB).

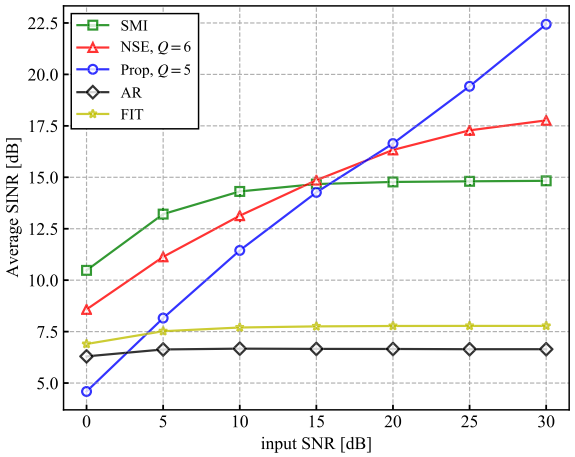

(a) Rayleigh fading channel.

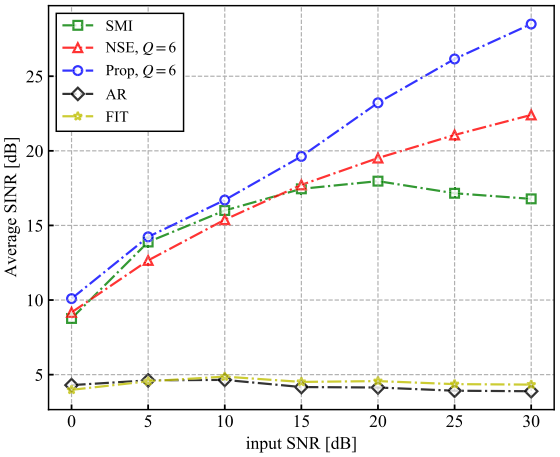

(b) Rician fading channel.

FIGURE 10. Time-averaged SINR per subframe versus input SNR (v = 10 km/h, SIR = 0 dB).

of the proposed scheme is the best at all SNR region in Rician fading channel.

Table 4 summarized possible schemes that provided significant performance as output SINR for each environmental parameter. From Figs. 8a, 9a, and 10a, the proposed scheme in Rayleigh fading channel is effective at a low speed, low SIR, and high SNR environment. On the other hand, from Figs. 8b, 9b, and 10b, its effectiveness in Rician fading channel can be further extended to almost all conditions. In the small cell scenario of 5G systems with millimeter-wave bands, the possible channel environment is considered to be Rician with spatially correlated. We can conclude that the proposed scheme could be an essential solution for ultimate high capacity multiuser MIMO transmission in a mobility environment towards 5G and beyond systems.

TABLE 4. Comparison results with parameters.

	Rayleigh		Rician	
	Low	High	Low	High
Moving speed	Prop.	SMI, AR	Prop.	Prop.
Input SIR	Prop.	NSE	Prop.	NSE, Prop.
Input SNR	SMI	Prop.	Prop.	Prop.

C. DISCUSSION AND FUTURE WORK

The above evaluations are performed assuming a narrow band single-carrier basis. The proposed scheme can also be extended to the wideband communication scheme such as OFDM; it can be simply applied per subcarrier. Besides, the simulation assumed 8 desired users and 2 interfering users in the area of interest. Even though the number of users increases, the proposed scheme is still applicable as long as the total number of users or signal streams to be multiplexed is less than DoFs available. As shown in Fig. 7a, Q has an optimal value depending on the user velocity. In this article, we treated Q as a fixed parameter in the conventional NSE and the proposed schemes in order to analyze its dependency. One

possible approach to find the optimal value of Q is recently conceived using principal component analysis of expanded channel matrix [34]. By observing the singular values of the autocorrelation matrix $\sum_{q=0}^{Q-1} \mathbf{R}_{\mathbf{yy}}^{(n-q)}$, we can estimate the effective dimension of the time-varying interference channel vector space, that is, optimal value of Q. As disclosed in [34], since it is beyond the scope of this article to include the analysis results, the optimization of Q is a subject for future work to be combined.

Recent trend is to employ a neural network which has high versatility for wireless physical signal processing [35]–[37]. It will also be helpful for our proposal to find the optimal null-space from trained network via past channel transition. We should seek its applicability to boost up this new paradigm which could exceed the limitation of traditional signal processing. Moreover, channel prediction based approaches as a comparison in the evaluation and our NSE based one can be combined to further enhance output SINR performance as presented in [38]. This advanced scheme was developed for downlink, and hence modification specialized for uplink is also one of our study topics of interest.

V. CONCLUSION

This article proposed a novel interference suppression scheme for uplink multiuser massive MIMO systems based on null-space expansion and MMSE-SMI algorithm, under the time-varying channel environment as well as unknown interference existence. Vulnerability for spatial multiplexing due to user mobility can be resolved by exploiting past pilot sequences to steer multiple nulls for including future interference channels. Further, incorporating the SMI weight derivation principle can suppress not only IUI in the target cell but also unknown interferences such as ICI from adjacent cells. The proposed approach is also computationally efficient compared to the conventional NSE scheme. Computer simulations revealed that excellent interference suppression capability of the proposed scheme other than conventional schemes while allowing desired signal power loss. It is particularly effective in the region where large SNR and small SIR, well representing small cell and cell-free deployment scenarios. We can conclude that the proposed scheme is believed to be one of the promising approaches to realize interference free mobile communication enabled by massive array transceiver architecture.

APPENDIX

PROOF OF PROPERTY OF THE PROPOSED SCHEME

We prove the property (27) and (28) under the assumption that $\mathbf{N}^{(n)} = \mathbf{O}_{N_\mathrm{r}\times N_\mathrm{p}}$ and $(N_\mathrm{d} + N_\mathrm{i}) \leqq N_\mathrm{p}$ in (8). We define the extended channel matrix $\mathbf{H}_\mathrm{e}^{(n)} \in \mathbb{C}^{N_\mathrm{r}\times Q(N_\mathrm{d}+N_\mathrm{i})}$ and the extended transmission signal matrix $\mathbf{X}_\mathrm{e}^{(n)} \in \mathbb{C}^{Q(N_\mathrm{d}+N_\mathrm{i})\times QN_\mathrm{p}}$ in the n-th subframe as

$$\mathbf{H}_\mathrm{e}^{(n)} = \left[\, \mathbf{H}^{(n)} \;\; \mathbf{H}^{(n-1)} \;\; \cdots \;\; \mathbf{H}^{(n-Q+1)} \right] \tag{40}$$

$$\mathbf{X}_\mathrm{e}^{(n)} = \begin{bmatrix} \mathbf{X}^{(n)} & & & \mathbf{O} \\ & \mathbf{X}^{(n-1)} & & \\ & & \ddots & \\ \mathbf{O} & & & \mathbf{X}^{(n-Q+1)} \end{bmatrix} \tag{41}$$

where $\mathbf{H}^{(n-q)} = \left[\mathbf{H}_\mathrm{d}^{(n-q)} \;\; \mathbf{H}_\mathrm{i}^{(n-q)}\right] \in \mathbb{C}^{N_\mathrm{r}\times(N_\mathrm{d}+N_\mathrm{i})}$ is the channel matrix containing both the desired user and the interfering user channel matrix in the $(n-q)$-th subframe, and $\mathbf{X}^{(n-q)} = \left[\mathbf{X}_\mathrm{d}^{(n-q)T} \;\; \mathbf{X}_\mathrm{i}^{(n-q)T}\right]^T \in \mathbb{C}^{(N_\mathrm{d}+N_\mathrm{i})\times N_\mathrm{p}}$ is the transmission signal matrix containing both the desired and the interfering users' transmission signal matrix in the $(n-q)$-th subframe. The extended transmission signal matrix $\mathbf{X}_\mathrm{e}^{(n)}$ defined in (41) and the extended pilot signal matrix $\mathbf{X}_\mathrm{de}^{(n)}$ defined in (21) have the following relationship.

$$\mathbf{X}_\mathrm{de}^{(n)} = \mathbf{T}\mathbf{X}_\mathrm{e}^{(n)} \tag{42}$$

where $\mathbf{T} = \left[\left[\mathbf{I}_{N_\mathrm{d}}, \mathbf{O}_{N_\mathrm{d}\times N_\mathrm{i}}\right]\left[\mathbf{I}_{N_\mathrm{d}}, \mathbf{O}_{N_\mathrm{d}\times N_\mathrm{i}}\right]\cdots\left[\mathbf{I}_{N_\mathrm{d}}, \mathbf{O}_{N_\mathrm{d}\times N_\mathrm{i}}\right]\right] \in \mathbb{C}^{N_\mathrm{d}\times Q(N_\mathrm{d}+N_\mathrm{i})}$ is transformation matrix between $\mathbf{X}_\mathrm{e}^{(n)}$ and $\mathbf{X}_\mathrm{de}^{(n)}$. From (40) and (41), the extended received signal matrix $\mathbf{Y}_\mathrm{e}^{(n)}$ defined in (20) represents as follows.

$$\mathbf{Y}_\mathrm{e}^{(n)} = \mathbf{H}_\mathrm{e}^{(n)}\mathbf{X}_\mathrm{e}^{(n)} \tag{43}$$

Let the singular value decomposition of $\mathbf{Y}_\mathrm{e}^{(n)}$ be

$$\mathbf{Y}_\mathrm{e}^{(n)} = \left[\, \mathbf{U}_\mathrm{S} \;\; \mathbf{U}_\mathrm{N}\right] \begin{bmatrix} \Sigma_\mathrm{S} & \mathbf{O} \\ \mathbf{O} & \mathbf{O} \end{bmatrix} \begin{bmatrix} \mathbf{V}_\mathrm{S}^H \\ \mathbf{V}_\mathrm{N}^H \end{bmatrix} = \mathbf{U}\Sigma\mathbf{V}^H \tag{44}$$

where $\Sigma_\mathrm{S} \in \mathbb{C}^{Q(N_\mathrm{d}+N_\mathrm{i})\times Q(N_\mathrm{d}+N_\mathrm{i})}$ is a diagonal matrix with $Q(N_\mathrm{d}+N_\mathrm{i})$ singular values on the diagonal. $\mathbf{U}_\mathrm{S} \in \mathbb{C}^{N_\mathrm{r}\times Q(N_\mathrm{d}+N_\mathrm{i})}$ and $\mathbf{V}_\mathrm{S} \in \mathbb{C}^{QN_\mathrm{p}\times Q(N_\mathrm{d}+N_\mathrm{i})}$ are the set of left and right singular vectors corresponding to the $Q(N_\mathrm{d}+N_\mathrm{i})$ singular values. On the assumption that $\mathbf{H}_\mathrm{e}^{(n)}$ is a full column rank and $\mathbf{X}_\mathrm{e}^{(n)}$ is a full row rank, $\mathbf{H}_\mathrm{e}^{(n)}$ and $\mathbf{X}_\mathrm{e}^{(n)}$ can be transformed as follows.

$$\mathbf{H}_\mathrm{e}^{(n)} = \left[\, \mathbf{U}_\mathrm{S} \;\; \mathbf{U}_\mathrm{N}\right] \begin{bmatrix} \mathbf{A}_\mathrm{S} \\ \mathbf{O} \end{bmatrix} = \mathbf{U}\mathbf{A} \tag{45}$$

$$\mathbf{X}_\mathrm{e}^{(n)} = \left[\, \mathbf{B}_\mathrm{S} \;\; \mathbf{O}\right] \begin{bmatrix} \mathbf{V}_\mathrm{S}^H \\ \mathbf{V}_\mathrm{N}^H \end{bmatrix} = \mathbf{B}\mathbf{V}^H \tag{46}$$

where the k-th column vector of $\mathbf{A}_\mathrm{S}$ is the coordinate of the k-th column vector of $\mathbf{H}_\mathrm{e}^{(n)}$ as measured by the basis $\mathbf{U}_\mathrm{S} = \left[\mathbf{u}_1\, \mathbf{u}_2\, \cdots\, \mathbf{u}_{Q(N_\mathrm{d}+N_\mathrm{i})}\right]$, and the k-th row vector of $\mathbf{B}_\mathrm{S}$ is the coordinate of the k-th row vector of $\mathbf{X}_\mathrm{e}^{(n)}$ as measured by the basis $\mathbf{V}_\mathrm{S}^* = \left[\mathbf{v}_1^*\, \mathbf{v}_2^*\, \cdots\, \mathbf{v}_{Q(N_\mathrm{d}+N_\mathrm{i})}^*\right]$. The former full column rank assumption means that the time-varying channel vectors are linearly independent at past Q time instants. The latter full row rank assumption means that the transmitted signal sequence of all users included interfering users are linearly independent in the pilot part.

Substituting (45), (46) into (43), we have

$$\mathbf{Y}_\mathrm{e}^{(n)} = \mathbf{U}\mathbf{A}\mathbf{B}\mathbf{V}^H \tag{47}$$

Since $\mathbf{U}$ and $\mathbf{V}$ are non singular matrices, the following relationship can be obtained by comparing (44) with (47).

$$\mathbf{A}\mathbf{B} = \Sigma \tag{48}$$

The postcoding weight $\mathbf{W}_{\text{prop}}^{(n)}$ defined by (25) is represented using (44) as follows.

$$\mathbf{W}_{\text{prop}}^{(n)} = \mathbf{U}\mathbf{K}\mathbf{V}^H\mathbf{X}_{\text{de}}^{(n)H} \tag{49}$$

where $\mathbf{K} = \begin{bmatrix} \Sigma_{\text{S}}^{-1} & \mathbf{O} \\ \mathbf{O} & \mathbf{O} \end{bmatrix} \in \mathbb{C}^{N_{\text{r}} \times QN_{\text{p}}}$ is diagonal matrix with the inverse of singular values in the diagonal elements. From (48) the following relationship between $\mathbf{K}$, $\mathbf{A}$, and $\mathbf{B}$ is established.

$$\mathbf{B}\mathbf{K}^H\mathbf{A} = \mathbf{I}_{Q(N_{\text{d}}+N_{\text{i}})} \tag{50}$$

Finally, from the (42), (45), (46), (49) (50), the following property can be obtained.

$$\mathbf{W}_{\text{prop}}^{(n)H}\mathbf{H}_{\text{e}}^{(n)} = \mathbf{T} \tag{51}$$

From the above (51), we see that the postcoding weight $\mathbf{W}_{\text{prop}}^{(n)}$ satisfies the following property.

$$\begin{aligned} \mathbf{W}_{\text{prop}}^{(n)H}\mathbf{H}_{\text{d}}^{(n-q)} &= \mathbf{I}_{N_{\text{d}}} \\ \mathbf{W}_{\text{prop}}^{(n)H}\mathbf{H}_{\text{i}}^{(n-q)} &= \mathbf{O}_{N_{\text{d}} \times N_{\text{i}}}, \quad \text{for } q = 0,\ 1,\ \ldots,\ Q-1 \end{aligned}$$

REFERENCES

[1] J. G. Andrews, S. Buzzi, W. Choi, S. V. Hanly, A. Lozano, A. C. K. Soong, and J. C. Zhang, "What will 5G be?" *IEEE J. Sel. Areas Commun.*, vol. 32, no. 6, pp. 1065–1082, Jun. 2014.

[2] A. L. Swindlehurst, E. Ayanoglu, P. Heydari, and F. Capolino, "Millimeter-wave massive MIMO: The next wireless revolution?" *IEEE Commun. Mag.*, vol. 52, no. 9, pp. 56–62, Sep. 2014.

[3] E. G. Larsson, O. Edfors, F. Tufvesson, and T. L. Marzetta, "Massive MIMO for next generation wireless systems," *IEEE Commun. Mag.*, vol. 52, no. 2, pp. 186–195, Feb. 2014.

[4] K. Maruta, A. Ohta, S. Kurosaki, T. Arai, and M. Iizuka, "Experimental investigation of space division multiplexing on massive antenna systems," in *Proc. IEEE Int. Conf. Commun. (ICC)*, Jun. 2015, pp. 2042–2047.

[5] Q. H. Spencer, C. B. Peel, A. L. Swindlehurst, and M. Haardt, "An introduction to the multi-user MIMO downlink," *IEEE Commun. Mag.*, vol. 42, no. 10, pp. 60–67, Oct. 2004.

[6] C. Sun, X. Gao, S. Jin, M. Matthaiou, Z. Ding, and C. Xiao, "Beam division multiple access transmission for massive MIMO communications," *IEEE Trans. Commun.*, vol. 63, no. 6, pp. 2170–2184, Jun. 2015.

[7] B. Mondal, V. Sergeev, A. Sengupta, G. Ermolaev, A. Davydov, E. Kwon, S. Han, and A. Papathanassiou, "MU-MIMO and CSI feedback performance of NR/LTE," in *Proc. 53rd Annu. Conf. Inf. Sci. Syst. (CISS)*, Mar. 2019, pp. 1–6.

[8] H. P. Bui, Y. Ogawa, T. Nishimura, and T. Ohgane, "Performance evaluation of a multi-user MIMO system with prediction of time-varying indoor channels," *IEEE Trans. Antennas Propag.*, vol. 61, no. 1, pp. 371–379, Jan. 2013.

[9] K. E. Baddour and N. C. Beaulieu, "Autoregressive modeling for fading channel simulation," *IEEE Trans. Wireless Commun.*, vol. 4, no. 4, pp. 1650–1662, Jul. 2005.

[10] W. Peng, M. Zou, and T. Jiang, "Channel prediction in time-varying massive MIMO environments," *IEEE Access*, vol. 5, pp. 23938–23946, 2017.

[11] T. Iwakuni, K. Maruta, A. Ohta, Y. Shirato, T. Arai, and M. Iizuka, "Inter-user interference suppression in time varying channel with null-space expansion for multiuser massive MIMO," in *Proc. IEEE 26th Annu. Int. Symp. Pers., Indoor, Mobile Radio Commun. (PIMRC)*, Aug. 2015, pp. 558–562.

[12] T. Iwakuni, K. Maruta, A. Ohta, Y. Shirato, T. Arai, and M. Iizuka, "Null-space expansion for multiuser massive MIMO inter-user interference suppression in time varying channels," *IEICE Trans. Commun.*, vol. E100.B, no. 5, pp. 865–873, 2017.

[13] T. L. Marzetta, "Noncooperative cellular wireless with unlimited numbers of base station antennas," *IEEE Trans. Wireless Commun.*, vol. 9, no. 11, pp. 3590–3600, Nov. 2010.

[14] J. Jose, A. Ashikhmin, T. L. Marzetta, and S. Vishwanath, "Pilot contamination and precoding in multi-cell TDD systems," *IEEE Trans. Wireless Commun.*, vol. 10, no. 8, pp. 2640–2651, Aug. 2011.

[15] B. Widrow, P. E. Mantey, L. J. Griffiths, and B. B. Goode, "Adaptive antenna systems," *Proc. IEEE*, vol. 55, no. 12, pp. 2143–2159, Dec. 1967.

[16] D. Tokuyasu, M. Taromaru, R. Ono, and M. Ohta, "A study on propagation model and mechanism on null-space dimension expansion for multi-user MIMO tolerant to channel fluctuation," in *Proc. Int. Workshop Smart Wireless Commun. (SmartCom)*, vol. 116, no. 29, 2016, pp. 73–74.

[17] H. Ban, D. Motegi, M. Taromaru, and M. Ohta, "A study on beam pattern of array with multi-user MIMO using null-space expansion tolerant to channel fluctuation," in *Proc. Int. Workshop Smart Wireless Commun. (SmartCom)*, vol. 117, no. 257, 2017, pp. 63–64.

[18] T. Taniguchi, Y. Karasawa, and N. Nakajima, "Performance analysis of multiuser MIMO system based on zero forcing for moving targets," in *Proc. 10th Eur. Conf. Antennas Propag. (EuCAP)*, Apr. 2016, pp. 1–5.

[19] T. Taniguchi, Y. Karasawa, and N. Nakajima, "Performance analysis of zero forcing based multiuser MIMO downlink system under time variant channels," *IEICE Commun. Express*, vol. 5, no. 5, pp. 124–128, 2016.

[20] T. Iwakuni, K. Maruta, A. Ohta, Y. Shirato, T. Arai, and M. Iizuka, "Experimental verification of null-space expansion for multiuser massive MIMO using measured channel state information," in *Proc. IEEE 84th Veh. Technol. Conf. (VTC-Fall)*, Sep. 2016, pp. 1–5.

[21] T. Iwakuni, K. Maruta, A. Ohta, Y. Shirato, and M. Iizuka, "Experimental verification of null-space expansion for multiuser massive MIMO via channel state information measurement," *IEICE Trans. Commun.*, vol. E101.B, no. 3, pp. 877–884, 2018.

[22] H. Q. Ngo and E. G. Larsson, "EVD-based channel estimation in multicell multiuser MIMO systems with very large antenna arrays," in *Proc. IEEE Int. Conf. Acoust., Speech Signal Process. (ICASSP)*, Mar. 2012, pp. 3249–3252.

[23] K. Maruta and C.-J. Ahn, "Uplink interference suppression by semi-blind adaptive array with decision feedback channel estimation on multicell massive MIMO systems," *IEEE Trans. Commun.*, vol. 66, no. 12, pp. 6123–6134, Dec. 2018.

[24] K. Maruta and C.-J. Ahn, "Improving semi-blind uplink interference suppression on multicell massive MIMO systems: A beamspace approach," *IEICE Trans. Commun.*, vol. E102.B, no. 8, pp. 1503–1511, 2019.

[25] M. K. Ozdemir and H. Arslan, "Channel estimation for wireless OFDM systems," *IEEE Commun. Surveys Tuts.*, vol. 9, no. 2, pp. 18–48, 2nd Quart., 2007.

[26] R. K. Patra and C. K. Nayak, "A comparison between different adaptive beamforming techniques," in *Proc. Int. Conf. Range Technol. (ICORT)*, Feb. 2019, pp. 1–4.

[27] S. Zhu, T. S. Ghazaany, S. M. R. Jones, R. A. Abd-Alhameed, J. M. Noras, T. Van Buren, J. Wilson, T. Suggett, and S. Marker, "Probability distribution of rician K-factor in urban, suburban and rural areas using real-world captured data," *IEEE Trans. Antennas Propag.*, vol. 62, no. 7, pp. 3835–3839, Jul. 2014.

[28] K. Yu, M. Bengtsson, B. Ottersten, D. McNamara, P. Karlsson, and M. Beach, "Modeling of wide-band MIMO radio channels based on NLoS indoor measurements," *IEEE Trans. Veh. Technol.*, vol. 53, no. 3, pp. 655–665, May 2004.

[29] W. C. Jakes, *Microwave Mobile Communications*. Piscataway, NJ, USA: IEEE Press, 1974.

[30] *Study on Channel Model for Frequencies From 0.5 to 100 Ghz (Release 16)*, Standard 3GPP TR 38.901 version 14.0.0 Release 14, 3rd Generation Partnership Project (3GPP), Tech. Rep., Dec. 2019.

[31] Q. H. Spencer, A. L. Swindlehurst, and M. Haardt, "Zero-forcing methods for downlink spatial multiplexing in multiuser MIMO channels," *IEEE Trans. Signal Process.*, vol. 52, no. 2, pp. 461–471, Feb. 2004.

[32] D. Tse and P. Viswanath, *Fundamentals of Wireless Communication*. Cambridge, U.K.: Cambridge Univ. Press, 2005.

[33] E. Kunnari and J. Iinatti, "Stochastic modelling of Rice fading channels with temporal, spatial and spectral correlation," *IET Commun.*, vol. 1, no. 2, pp. 215–224, Apr. 2007.

[34] N. Funaki, K. Maruta, and C. Ahn, "Improved null-space expansion scheme under presence of channel estimation error for multiuser massive MIMO," in *Proc. 23rd Int. Symp. Wireless Pers. Multimedia Commun. (WPMC)*, 2020.

[35] C. Huang, G. C. Alexandropoulos, A. Zappone, C. Yuen, and M. Debbah, "Deep learning for UL/DL channel calibration in generic massive MIMO systems," in *Proc. IEEE Int. Conf. Commun. (ICC)*, May 2019, pp. 1–6.

[36] S. Kojima, K. Maruta, and C.-J. Ahn, "Adaptive modulation and coding using neural network based SNR estimation," *IEEE Access*, vol. 7, pp. 183545–183553, Dec. 2019.
[37] T. Omura, S. Kojima, K. Maruta, and C.-J. Ahn, "Neural network based channel identification and compensation," *IEICE Commun. Express*, vol. 8, no. 10, pp. 416–421, Oct. 2019.
[38] K. Arai, K. Maruta, and C. Ahn, "High beamforming gain precoding weight design scheme with null-space expansion for multiuser massive MIMO in time-varying channels," in *Proc. 23rd Int. Symp. Wireless Pers. Multimedia Commun. (WPMC)*, Oct. 2020.

KABUTO ARAI (Graduate Student Member, IEEE) received the B.E. degree in electrical and electronics engineering from Chiba University, Japan, in 2019, where he is currently pursuing the M.E. degree with the Graduate School of Engineering. His research interests include MIMO, channel estimation, and adaptive array signal processing.

KAZUKI MARUTA (Member, IEEE) received the B.E., M.E., and Ph.D. degrees in engineering from Kyushu University, Japan, in 2006, 2008, and 2016, respectively. From 2008 to 2017, he was with NTT Access Network Service Systems Laboratories and was engaged in the research and development of interference compensation techniques for future wireless communication systems. From 2017 to 2020, he was an Assistant Professor with the Graduate School of Engineering, Chiba University. He is currently a Specially Appointed Associate Professor with the Academy for Super Smart Society, Tokyo Institute of Technology. His research interests include MIMO, adaptive array signal processing, channel estimation, medium access control protocols, and moving networks. He is a member of The Institute of Electronics, Information and Communication Engineers (IEICE). He received the IEICE Young Researcher's Award in 2012, the IEICE Radio Communication Systems (RCS) Active Researcher Award in 2014, the APMC2014 Prize, and the IEICE RCS Outstanding Researcher Award in 2018. He was a co-recipient of the IEICE Best Paper Award in 2018, the SoftCOM2018 Best Paper Award, and the APCC2019 Best Paper Award.

CHANG-JUN AHN (Senior Member, IEEE) received the Ph.D. degree from the Department of Information and Computer Science, Keio University, Japan, in 2003. From 2001 to 2003, he was a Research Associate with the Department of Information and Computer Science, Keio University. From 2003 to 2006, he was with the Communication Research Laboratory, Independent Administrative Institution (now the National Institute of Information and Communications Technology). In 2006, he was on assignment at ATR Wave Engineering Laboratories. In 2007, he was a Lecturer with the Faculty of Information Sciences, Hiroshima City University. He is currently a Professor with the Graduate School of Engineering, Chiba University. His research interests include OFDM, MIMO, digital communication, channel coding, signal processing for telecommunications, and wireless power transfer. He is a Senior Member of IEICE. From 2005 to 2006, he was an Expert Committee Member of Emergence Communication Committee, Shikoku Bureau of Telecommunications, Ministry of Internal Affairs and Communications (MIC), Japan. He received the ICF Research Grant Award for Young Engineer in 2002, the Funai Information Science Award for Young Scientist in 2003, and the Distinguished Service Award from Hiroshima City in 2010. He once served as an Associate Editor for Special Section on Multi-Dimensional Mobile Information Network for the *IEICE Transactions on Fundamentals*.